



Form and function of tentacles in pteriomorphian bivalves

Journal:	<i>Journal of Morphology</i>
Manuscript ID	JMOR-19-0167.R1
Wiley - Manuscript type:	Research Article
Date Submitted by the Author:	n/a
Complete List of Authors:	Audino, Jorge; Universidade de São Paulo Instituto de Biociências, Department of Zoology Marian, José Eduardo; Universidade de São Paulo Instituto de Biociências, Department of Zoology
Keywords:	anatomy, invertebrates, microscopy, secretory, sensory

SCHOLARONE™
Manuscripts

1
2
3
4
5
6
7
8
9
10
11
12
13
14
15
16
17
18
19
20
21
22
23
24
25
26
27
28
29
30
31
32
33
34
35
36
37
38
39
40
41
42
43
44
45
46
47
48
49
50
51
52
53
54
55
56
57
58
59
60

1 **Title: Form and function of tentacles in pteriomorphian bivalves**

2

3 Running title: Tentacles in pteriomorphian bivalves

4

5 Authors: Jorge Alves Audino and José Eduardo Amoroso Rodriguez Marian

6

7 Address: Department of Zoology, University of São Paulo, Rua do Matão, Travessa 14,
8 n. 101, 05508-090 São Paulo, São Paulo, Brazil

9

10 Corresponding author: J. A. Audino

11 E-mail: jorgeaudino@ib.usp.br

12 ORCID: 0000-0002-9688-559X

13

14 José E. A. R. Marian – jemarian@ib.usp.br – ORCID: 0000-0001-7894-0391

15

16

17

18 Abstract

19 Tentacles are remarkable anatomical structures in **invertebrates** for their
20 diversity of form and function. In bivalves, tentacular organs are commonly associated
21 with protective, secretory, and sensory roles. However, anatomical details are available
22 for only a few species, rendering the diversity and evolution of bivalve tentacles still
23 obscure. In Pteriomorphia, a clade including oysters, scallops, pearl oysters, and
24 relatives, tentacles are abundant and diverse. We investigated tentacle anatomy in the
25 group to understand variation, infer functions, and investigate patterns in tentacle
26 diversity. Six species from four pteriomorphian families (Ostreidae, Pinnidae, Pteriidae,
27 Spondylidae) were collected and thoroughly investigated **with** integrative microscopy
28 techniques, including histology, scanning electron microscopy, and confocal
29 microscopy. Tentacles can be **classified as** middle fold tentacles (MFT) and inner fold
30 tentacles (IFT) according to their position **with respect to the folds of the mantle margin**.
31 While MFT morphology indicates intense secretion of mucosubstances, no evidence for
32 secretory activity was found for IFT. However, both tentacle types have **appropriate**
33 ciliary **distribution and length** to promote mucus transportation for cleaning and
34 lubrication. Protective and sensory functions are discussed based on different lines of
35 evidence, including secretion, cilia distribution, musculature, and innervation. Our
36 results support the **homology of MFT and IFT only for Pterioidea and Ostreioidea**,
37 considering their morphology, presence of ciliated receptors at the **tips**, and branched
38 innervation pattern. This is in accordance with recent phylogenetic hypotheses that
39 support the close relationship between **these** superfamilies. In contrast, major structural
40 differences indicate that MFT and IFT are probably not homologous across all
41 pteriomorphians. By applying integrative microscopy, we were able to reveal

1
2
3
4 42 anatomical elements that are essential for the understanding of homology and function
5
6 43 when dealing with such superficially similar structures.
7
8

9 44

10
11 45 **Keywords:** anatomy, invertebrates, mantle, microscopy, molluscs, secretory, sensory.
12

13 46

14
15 47

16
17
18 48 **Research Highlights**

19
20 49 Detailed microscopical analysis of tentacles in pteriomorphian bivalves not only
21
22 50 provided anatomical evidence to describe the functional morphology of such diverse
23
24 51 organs, but also revealed possible shared traits for the clades Pterioidea and Ostreoidea.
25
26

27 52

28
29 53
30
31
32
33
34
35
36
37
38
39
40
41
42
43
44
45
46
47
48
49
50
51
52
53
54
55
56
57
58
59
60

54 1. Introduction

55 Tentacular organs, including palps, tentacles, and papillae, are among key
56 features in the taxonomy and biology of most invertebrate groups. Tentacles may be
57 generically defined as slender, flexible appendages in animals, usually comprehending
58 contractible, **soft-tissue** extensions of the body (Brusca, Moore, & Shuster, 2016).
59 Despite clearly not **being** homologous between phyla, tentacles have evolved **multiple**
60 **times** in numerous taxa, performing different roles deeply associated with the lifestyle
61 and **ecology** of the organism (Roberts & Moore, 1997; Zhadan & Tzetlin, 2002;
62 Audino, Marian, Wanninger, & Lopes, 2015; Tamberg & Shunatova, 2017). In this
63 context, three main functions can be assigned to tentacular organs, i.e., feeding,
64 protective, and sensory.

65 In several invertebrate species, tentacles are related to feeding behavior through
66 the collection of food particles by ciliary mechanisms. In sea cucumbers and
67 sipunculans, for example, the oral tentacles are used in nonselective deposit feeding, or
68 water filtering, by means of a combination of hydrostatic pressure, complex
69 musculature, and mucus coating (Cameron & Fankboner, 1984; Pilger, 1982). In most
70 suspension feeders, such as bryozoans, phoronids, entoprocts, and many polychaetes,
71 tentacles **are organized** in crowns responsible for both water flow and food particle
72 collection by mucociliary transportation (Dubois, Barillé, Cognie, & Beninger, 2005;
73 Nielsen & Riisgård, 1998; Riisgård, 2002; Schwaha & Wanninger, 2015; Tamberg &
74 Shunatova, 2016, 2017).

75 In cnidarians, tentacle crowns are commonly found around the mouth **of a polyp**
76 or at the edge of the umbrella in medusae (Shimizu & Namikawa, 2009). In anemones,
77 corals, and tube anemones, tentacles bear a great diversity of nematocysts and

1
2
3
4 78 spirocysts, the former used for stinging and capturing prey, while the latter are used for
5
6 79 binding the prey to the feeding tentacles (Rifkin, 1991; Thorington & Hessinger, 1998).
7
8
9 80 Among cephalopod mollusks, nautilids use a complex adhesive gland system in the
10
11 81 digital tentacles to catch and bind the prey (von Byern, Wani, Schwaha, Grunwald, &
12
13 82 Cyran, 2012).

15 83 Tentacles can also be used in aggressive interactions or protective strategies. In
16
17 84 many anemones and antiphatarian corals, specialized tentacles are developed in
18
19 85 response to other cnidarian species, frequently resulting in extensive nematocyst
20
21 86 discharge (Goldberg, Grange, Taylor, & Zuniga, 1990; Watson & Mariscal, 1983). An
22
23 87 alternative form of protection can involve tentacle autotomy, as observed in some
24
25 88 medusae, preventing damage caused by tentacle entanglement with prey, predators, or
26
27 89 conspecifics (Bickell-Page & Mackie, 1991). In file clams (Limidae), specialized
28
29 90 tentacles are thought to be involved in protective responses through secretion of
30
31 91 distasteful substances (Gilmour, 1967).

32
33 92 In most mollusks, with the evident exception of cephalopods, tentacles are not
34
35 93 directly involved in feeding processes; instead, they participate in sensory roles. In
36
37 94 gastropods, for example, cephalic and mantle tentacles are sensory organs associated
38
39 95 with the acquisition of olfactory cues involved in a variety of social, feeding, and
40
41 96 reproductive behaviors (Croll, 1983; Künz & Haszprunar, 2001).

42
43 97 In many bivalve taxa, multiple tentacles are distributed along the mantle margin,
44
45 98 comprising an impressive diversity of form and function (Yonge, 1983). The bivalve
46
47 99 mantle is formed by left and right lobes, delimiting the mantle cavity, and their free
48
49 100 margins bear tissue extensions named mantle folds (Carter et al., 2012). Tentacles may
50
51 101 be present either on the middle mantle fold, on the inner mantle fold, or on both (Yonge,
52
53
54
55
56
57
58
59
60

1
2
3
4 102 1983). Within Bivalvia, the largest diversity of tentacles is found within the
5
6
7 103 Pteriomorpha. This large clade, which includes oysters, scallops, mussels, and
8
9 104 relatives, are characteristic for their numerous tentacles along the mantle margin. In
10
11 105 scallops (Pectinidae), long tentacles have been thoroughly examined for two species,
12
13 106 *Nodipecten nodosus* (Linnaeus, 1758) and *Placopecten magellanicus* (Gmelin, 1791),
14
15 107 and revealed to be specialized sensory organs (Audino et al., 2015; Moir, 1977).
16
17
18 108 Enormous tentacles are also present in Limidae, possibly performing sensory roles
19
20 109 (Gilmour, 1963, 1967). Tentacle morphology and distribution have been examined in
21
22 110 pearl oysters and relatives (Pterioidea), revealing shared attributes, such as tentacle
23
24 111 presence on two mantle folds and distribution along the entire mantle margin (Tëmkin,
25
26 112 2006).

27
28
29 113 Tentacular organs are an interesting system to be explored in the light of
30
31 114 multidisciplinary approaches investigating evolutionary novelties and the evolution of
32
33 115 complex phenotypes. As illustrated above, tentacles comprise key anatomical features to
34
35 116 understand the diversification of form and function. However, externally they are all
36
37 117 superficially similar, which requires a detailed anatomical investigation to detect
38
39 118 variation. In this study, we have applied integrative microscopy techniques to
40
41 119 investigate the functional anatomy of tentacles in representatives of major
42
43 120 pteriomorphian lineages, aiming at understanding variation, inferring functions, and
44
45 121 investigating patterns in tentacle diversity.
46
47
48
49

50 122

51 123 **2. Material and methods**

52
53 124 *Taxa sampling*
54
55
56
57
58
59
60

1
2
3
4 125 Samples were obtained for six pteriomorphians species collected during low tide
5
6 126 in São Sebastião's coast (State of São Paulo, Brazil): *Isognomon bicolor* (C. B. Adams,
7
8 127 1845), *Pinctada imbricata* Röding, 1798 and *Pteria colymbus* (Röding, 1798)
9
10 128 (Pteriidae), *Ostrea equestris* Say, 1834 (Ostreidae), *Pinna carnea* (Pinnidae), and
11
12 129 *Spondylus ictericus* Reeve, 1856 (Spondylidae). Sampled localities included rocky
13
14 130 shores (23°48'54.9"S 45°24'25.3"W, 23°49'44.7"S 45°26'29.6"W, 23°46'18.8"S
15
16 131 45°21'21.3"W) for *I. bicolor*, *Pi. imbricata*, *O. equestris*, and *S. ictericus*; gorgonian
17
18 132 clusters (23°49'40.5"S, 45°24'46.8"W) for *Pt. colymbus*; and sand flats (23°45'57.2"S
19
20 133 45°21'00.2"W) for *P. carnea*. Eight to ten individuals were collected per species, except
21
22 134 for *P. carnea* and *S. ictericus*, which included one specimen each. Mantle margin
23
24 135 samples were obtained after dissecting animals previously anesthetized in a 7.5%
25
26 136 solution of MgCl₂ for 3 h. Representatives of the Limidae and Pectinidae have been
27
28 137 previously examined (Audino et al., 2015; Gilmour, 1967) and were not included in our
29
30 138 study.

31
32
33
34
35
36 139 For histology and scanning electron microscopy (SEM), fragments of the mantle
37
38 140 margin bearing tentacles were fixed for 3 h at 4°C in a modified Karnovsky solution
39
40 141 (2.5% glutaraldehyde and 2% paraformaldehyde in 0.1 M sodium cacodylate buffer
41
42 142 with osmolarity adjusted to 1 Osm with sucrose), and stored in cacodylate buffer
43
44 143 (Audino & Marian, 2018). For confocal laser scanning microscopy (CLSM), samples
45
46 144 were fixed in 4% paraformaldehyde for 2 h and stored in 0.1 M phosphate buffer (PB)
47
48 145 (Audino & Marian, 2018).

49
50
51
52 146

53
54
55 147 *Microscopy techniques*

1
2
3
4 148 For scanning electron microscopy (SEM), **post-fixation** procedures were
5
6 149 conducted as described in Audino et al. (2015), **including 30 min in 1% OsO₄ in**
7
8 150 **cacodylate buffer, followed by 15 min in 1% tannic acid in buffer solution, and 15 min**
9
10 151 **in a fresh solution of 1% OsO₄ at 4°C**. Analysis and image acquisition were performed
11
12 152 on a Zeiss DSM 940. For confocal laser scanning microscopy (CLSM), samples were
13
14 153 permeabilized in PB containing 2% Triton-X 100 (PBT) overnight. To evidence
15
16 154 musculature, samples were incubated in a 1:40 dilution of Alexa Fluor 488 phalloidin
17
18 155 (Molecular Probes, USA) in PBT for 24 h at room temperature in the dark. For cilia and
19
20 156 nerve investigation, samples were incubated in a 1:400 dilution of alpha-tubulin
21
22 157 antibody (**monoclonal antibody, B-5-1-2**) with Alexa Fluor 488 conjugate (Molecular
23
24 158 Probes, USA) in the same conditions as described for phalloidin. After three washes of
25
26 159 15 min in PBT, samples were mounted **on** microscope slides in ProLong Diamond
27
28 160 Antifade Mountant with DAPI (Molecular Probes, USA). Analysis was performed on a
29
30 161 Zeiss LSM 880 (Zeiss, Germany) and image stacks were digitally merged in the
31
32 162 software ZEN lite 2.3 (Zeiss, Germany).

33
34
35
36
37
38
39 163 For histology, samples were completely dehydrated in ethanol and embedded in
40
41 164 resin (Leica HistoResin Kit, Germany). Serial sections of 4 µm were obtained **with** a
42
43 165 Leica RM2255 microtome (Leica, Germany). To evidence secretory cells, periodic acid-
44
45 166 Schiff stain (PAS) and alcian blue (AB) were applied for mucosubstances (Bancroft &
46
47 167 Stevens, 1982), and mercury-bromophenol blue (BB) was applied for protein aggregates
48
49 168 (Pearse, 1985). Other staining methods included hematoxylin and eosin (HE; Behmer et
50
51 169 al., 1976), Gomori trichrome stain (Humanson, 1962), and toluidine blue and basic
52
53 170 fuchsin (TF; Junqueira, 1995). The histological material and stubs (SEM) are deposited
54
55
56
57
58
59
60

1
2
3
4 171 at the Museum of Zoology 'Prof. Adão José Cardoso' of the State University of
5
6 172 Campinas (ZUEC, UNICAMP).
7
8

9 173

10 11 174 **3. Results**

12
13 175 In the studied animals, tentacles can be **classified** in two types according to their
14
15 176 location in the mantle margin, i.e., in which mantle fold they are located. Inner fold
16
17 177 tentacles (IFT) are marginal projections of **the long inner fold**, varying from filiform to
18
19 178 flattened structures. Middle fold tentacles (MFT) can be marginal or submarginal
20
21 179 projections, usually organized in commarginal rows. Anatomical features of IFT and
22
23 180 MFT are described below for each **species studied** and summarized in Table 1. **In some**
24
25 181 **samples, including those of *I. bicolor*, *P. carnea* and *S. ictericus*, intense pigmentation**
26
27 182 **or ciliary abundance prevented observation of tentacular nerves by CLSM.**
28
29
30
31

32 183
33
34 184 *Pteria colymbus* (Pteriidae)

35
36 185 MFT are marginal structures, filiform and more pigmented (brownish) at the
37
38 186 base **than the tip** (Fig. 1a). MFT are distributed on the entire fold extension, being more
39
40 187 abundant ventrally, **where they are proportionally larger than those at the dorsal region.**
41
42 188 They display two main sizes, short **(ca. 1.25 mm)** and long **(ca. 2.5 mm)**, short tentacles
43
44 189 **being about half** of the size of the adjacent long tentacles (Fig. 1a). Two types of
45
46 190 subepithelial secretory cells are abundant in the MFT; one type has granular content
47
48 191 with affinity for eosin and BB (Fig. 1b, c) and the other for PAS and AB (Fig. 1d). The
49
50 192 tentacle epithelium is covered by tufts of short cilia (Fig. 1e) **that are** more densely
51
52 193 distributed at the tentacle's base. A cluster of long cilia is located at the tip of each
53
54 194 tentacle (Fig. 1f). MFT are very muscular structures with numerous longitudinal fibers
55
56
57
58
59
60

1
2
3
4 195 (Fig. 1g) continuous with the mantle radial muscles. Thin fibers also form a delicate
5
6 196 transverse musculature (Fig. 1g). MFT are provided with central nerves that branch
7
8
9 197 towards the tip (Fig. S1a).

10
11 198 IFT are marginal, slightly pigmented, and present along the entire margin. In the
12
13 199 anterior and posterior regions, they are filiform, short, appearing as small papillae (Fig.
14
15 200 1a). In contrast, IFT are longer (ca. 2.5 mm) and slightly flat in the ventral region,
16
17 201 mainly along the incurrent aperture (Fig. 1h). In this region, some IFT are branched
18
19 202 (Fig. 1h), reaching similar lengths as the MFT. Pigmentation is also more intense
20
21 203 ventrally, with brown, yellow, and white spots (Fig. 1h). Despite intense secretory
22
23 204 activity in the inner mantle fold (data not shown), gland cells were not identified in the
24
25 205 IFT. Each tentacle is densely covered by cilia, both in short non-branched (Fig. 1i) and
26
27 206 large branched tentacles (Fig. 1j, k). Isolated clusters of cilia were not observed at the
28
29 207 tip. Musculature in IFT is similar to MFT, including longitudinal and transverse fibers,
30
31 208 although muscle bundles ramify in branched tentacles (Fig. 1l). IFT innervation
32
33 209 includes multiple, branching tentacular nerves (Fig. S1b).
34
35
36
37
38
39
40

41 *Pinctada imbricata* (Pteriidae)

42
43 212 MFT are marginal, filiform, and pigmented at the base (brownish and greyish).
44
45 213 They are very similar to those observed in *Pt. colymbus*, including the presence of short
46
47 214 and long tentacles. In the ventral region, MFT are proportionally longer and more
48
49 215 abundant than those in the dorsal region. Intense secretory activity is suggested by
50
51 216 subepithelial secretory cells with affinity for PAS and AB (Fig. 2a). Affinity for eosin –
52
53 217 but not for BB – was also observed in other subepithelial cells. Each MFT has a cluster
54
55 218 of long cilia at the tip (Fig. 2b), while shorter cilia are sparsely distributed along the
56
57
58
59
60

1
2
3
4 219 tentacle. Longitudinal musculature runs along the lengths of the tentacles (Fig. 2c), but
5
6 220 transverse fibers were not observed. Innervation includes multiple, branching tentacular
7
8 221 nerves (Fig. S1c).

9
10
11 222 IFT are marginal and slightly pigmented along the entire margin, including
12
13 223 white spots. They are longer and wider ventrally (ca. 3 mm long), especially along the
14
15 224 incurrent aperture, where most of them are branched and slightly flat (Fig. 2d). In
16
17
18 225 general, tissue organization of IFT is similar to the that of the inner fold, except for the
19
20 226 absence of secretory cells in the former (Fig. 2e). Tufts of cilia are sparsely distributed
21
22 227 on their surfaces (Fig. 2f, g), and a ciliary cluster is present at the tip of each branch
23
24 228 (Fig. 2h). The musculature is comprised of a few transverse fibers and numerous
25
26 229 longitudinal muscles, which ramify in branched tentacles. The nerves are highly
27
28 230 branched (Fig. 2h), even in non-branched tentacles, from the base to the tips. Small
29
30 231 nerves directly reach the ciliary tufts, especially those at the tips where numerous ciliary
31
32 232 roots and nerves appear to be connected (Fig. 2h).

33
34
35
36 233

37 38 39 234 *Isognomon bicolor* (Pteriidae)

40
41 235 MFT are marginal and filiform; pigmentation can vary from light to dark grey.
42
43 236 Along the entire margin, adjacent tentacles have similar sizes (from 0.5 to 1 mm),
44
45 237 although they are proportionally longer and more abundant in the ventral region. Intense
46
47 238 secretory activity should be present, evidenced by subepithelial secretory cells with
48
49 239 large granules with affinity for both eosin (Fig. 3a) and toluidine blue (stained in light
50
51 240 blue; Fig. 3b), but not for PAS or alcian blue (Fig. 3c). Epithelial secretory cells, in turn,
52
53 241 are evidenced by TF (stained in pink; Fig. 3b) and AB (Fig. 3c). Tentacles are densely
54
55 242 covered by cilia at their bases, but tufts are largely scarce on the inner surface (i.e., the
56
57
58
59
60

1
2
3
4 243 surface opposed to the valve) (Fig. 3d). A cluster of cilia is located at the tip (Fig. 3e).
5
6 244 Musculature includes transverse and longitudinal fibers, the latter being more developed
7
8 245 than the former (Fig. 3f). Innervation was not observed.

9
10
11 246 IFT are marginal, slightly flat, and darkly pigmented, although pigmentation is
12
13 247 less intense than the rest of the inner fold. Adjacent tentacles are similar in size (from
14
15 248 0.5 to 1 mm) and IFT are present along the entire margin, being longer ventrally and
16
17 249 non-branched. Secretory cells are lacking, and cilia cover the surfaces of the tentacles,
18
19 250 being more concentrated distally (Fig. 3g), where a cluster is present (Fig. 3h).
20
21 251 Musculature includes longitudinal and transverse fibers. Branched innervation seems
22
23 252 present, with nerves reaching the long ciliary roots at the tip (Fig. 3h).
24
25
26
27
28
29

30 254 *Ostrea equestris* (Ostreidae)

31
32 255 MFT are submarginal, filiform, and pigmented with brownish to grayish spots.
33
34 256 The position of the tentacles on the inner surface of the fold (i.e., the surface of the fold
35
36 257 opposed to the valve) includes distal and proximal commarginal rows. Shorter tentacles
37
38 258 (ca. 1 mm) are located on the distal row, near to the edge, while longer tentacles (ca. 2
39
40 259 mm) are proximal. In the ventral region, MFT are proportionally longer and more
41
42 260 abundant, particularly along the incurrent aperture. Short and long tentacles likely
43
44 261 display intense secretory activity, as indicated by subepithelial and epithelial secretory
45
46 262 cells. Two types of subepithelial secretory cells are present. Cells with more sparsely
47
48 263 distributed granules were stained in dark blue with toluidine blue (Fig. 4a) and had
49
50 264 affinity for BB (Fig. 4c); those with more densely distributed granules stained in light
51
52 265 blue with toluidine blue (Fig. 4a) and had a strong affinity for eosin (Fig. 4b). Weak
53
54 266 affinity for PAS and AB was observed for both cell types. Each MFT has abundant tufts
55
56
57
58
59
60

1
2
3
4 267 of cilia on its epithelium and a dense cluster of cilia at the tip (Fig. 4d, f). MFT are very
5
6 268 muscular; this system is dominated by longitudinal fibers (Fig. 4e). Tentacle innervation
7
8 269 is provided by branching nerves from the base reaching the ciliary rootlets, which are
9
10 270 more evident at the apical tufts (Fig. 4f).

11
12
13 271 IFT are marginal (Fig. 4g), filiform, usually lightly pigmented, and adjacent
14
15 272 tentacles are similar in size (ca. 1.5 mm). Along the margin, IFT are longer ventrally,
16
17 273 but never branched. Secretory cells were not detected. Cilia on the tentacle surface are
18
19 274 distributed in numerous longitudinal rows (Fig. 4h, i), forming a dense cluster at the tip
20
21 275 (Fig. 4j). Tentacle musculature is formed by longitudinal fibers, with no evidence of
22
23 276 transverse fibers (Fig. 4k). Innervation includes multiple branching nerves from the base
24
25 277 to the tip.

26
27
28
29 278

30
31
32 279 *Pinna carnea* (Pinnidae)

33
34 280 Only IFT are present. They are marginal, slightly flattened, and pigmentation
35
36 281 includes tiny yellow, brown, and whitish spots (Fig. 5a). IFT occur only in the posterior
37
38 282 region, being larger along the incurrent and excurrent apertures (Fig. 5a). Secretory cells
39
40 283 were not detected in histological sections, although droplets of possible mucosubstances
41
42 284 were observed interspersed with the short cilia that cover the entire tentacle surface
43
44 285 (Fig. 5b, c). No clusters of cilia were observed at the tentacle tips. Musculature is
45
46 286 formed by longitudinal and transverse fibers (Fig. 5d). Innervation was not observed.

47
48
49 287

50
51
52 288 *Spondylus ictericus* (Spondylidae)

53
54 289 MFT are submarginal, filiform, and slightly pigmented with yellow and whitish
55
56 290 spots (Fig. 6a). Brown and white pigmentation are more intense on the outer surface,
57
58
59
60

1
2
3
4 291 i.e., the side that faces the valve. MFT are located on the inner surface of the fold,
5
6 292 occupying proximal to distal positions (Fig. 6b). Some tentacles are modified as
7
8 293 eyestalks, bearing an eye at their tip (Fig. 6a). Extremely long tentacles (more than 5
9
10 294 mm) are also present in a proximal position on the fold, being much longer than
11
12 295 adjacent tentacles (ca. 2 mm) (Fig. 6a). MFT are uniformly distributed along the entire
13
14 296 margin, with no evident difference in density or size with body regions. The epithelium
15
16 297 contains numerous secretory cells stained by PAS and alcian blue (Fig. 6c), with low
17
18 298 affinity for TF and none for BB or eosin. Long tentacles show sparse tufts of cilia on the
19
20 299 epithelium (Fig. 6d), while the remaining tentacles have cilia organized in longitudinal
21
22 300 rows (Fig. 6e). No clusters of cilia were observed at the tentacle tips. Droplets of
23
24 301 mucosubstances were observed on the ciliary rows, possibly being secreted by the
25
26 302 adjacent glandular epithelium (Fig. 6f). Musculature and innervation could not be
27
28 303 investigated by confocal microscopy, but histological sections indicate abundance of
29
30 304 longitudinal and transverse fibers, as well as a central tentacular nerve (Fig. S1d).

31
32 305 IFT are very small marginal projections, similar to papillae (Fig. 6a). They are
33
34 306 uniformly distributed along the entire margin, being unpigmented and translucent. No
35
36 307 evidence for secretory activity was detected. Short cilia cover all tentacle surfaces while
37
38 308 long cilia are present in sparsely distributed tufts (Fig. 6g, h) but are not concentrated in
39
40 309 a cluster at the tip. Despite their small size, IFT are provided with longitudinal muscles
41
42 310 and tiny transverse muscle fibers (Fig. 6i). Innervation was not observed.

43
44
45
46
47
48
49
50
51
52 311

53 312 4. Discussion

54
55 313 *Gross-morphology and distribution of tentacles*
56
57
58
59
60

1
2
3
4 314 All species studied herein have tentacles on both mantle folds, except for *Pinna*
5
6 315 *carnea*, which has tentacles only on the inner fold. In addition, tentacles may be
7
8 316 distributed along the entire mantle margin or be restricted to some regions. The former
9
10 317 condition is observed in most studied species, with tentacle distribution along the
11
12 318 mantle extension. Nevertheless, tentacles are more abundant and larger ventrally in
13
14 319 pterioid and ostreoid species (Table 1). The latter condition is illustrated by *Pinna carnea*,
15
16 320 with tentacles restricted to the posterior region, bordering the **incurrent** and **excurrent**
17
18 321 apertures (Yonge, 1953).

22
23 322 In infaunal and semi-infaunal bivalves, IFT are common on the siphons as
24
25 323 sensory and protective structures distributed close to their apertures (Yonge, 1983). A
26
27 324 great diversity in shape and number of siphonal tentacles was described for infaunal
28
29 325 bivalves from the families Veneridae, Donacidae, and Tellinidae, which have multiple
30
31 326 branched tentacles on the **incurrent** siphon (Fishelson, 2000; Narchi, 1972; Piffer,
32
33 327 Arruda, & Passos, 2011; Sartori & Domaneschi, 2005; Sartori, Printrakoon, Mikkelsen,
34
35 328 & Bieler, 2008; Vitonis, Zaniratto, Machado, & Passos, 2012). Despite the absence of a
36
37 329 siphon, a similar condition is present in *Pteria colymbus* and *Pinctada imbricata* – both
38
39 330 species have well-developed, branched tentacles restricted to the ventral, **incurrent**
40
41 331 region. Carnivorous bivalves from the order Anomalodesmata also bear siphonal
42
43 332 tentacles (e.g., *Cardiomya cleryana*; Machado, Morton, & Passos, 2017). More rarely,
44
45 333 tentacles may also occur in the anterior portion of the pedal opening, as observed in
46
47 334 Cyammiidae (Passos & Machado, 2014).

52
53 335 Among the Pteriomorphia, tentacles have been studied in detail only for a few
54
55 336 species, although general observations were described for many groups (Waller, 1975).
56
57 337 In file clams (Limidae), MFT pigmentation ranges from translucent white to intense red.
58
59
60

1
2
3
4 338 In these bivalves, they vary from short to extremely long structures, sometimes
5
6 339 annulated, and always restricted to the middle fold, where they are usually densely
7
8 340 distributed (Allen, 2004; Gilmour, 1963, 1967; Mikkelsen & Bieler, 2003). In the
9
10 341 **Pectinoidea**, scallops (Pectinidae) and thorny oysters (Spondylidae) have MFT formed
11
12 342 on the inner surface of the middle fold (i.e., the surface opposed to the valve), also
13
14 343 including very long tentacles (Audino et al., 2015; Dakin, 1928b; Moir, 1977).
15
16 344 Tentacles on the inner mantle fold are also common in scallops; given that they are
17
18 345 located along the margin, they are named “guard tentacles” of the mantle cavity aperture
19
20 346 (Audino et al., 2015; Dakin, 1909; Drew, 1906). Although previous studies have not
21
22 347 recorded IFT in Spondylidae (Dakin, 1928a), our data for *Spondylus ictericus* show
23
24 348 robust evidence for their presence. Possibly due to their extremely small size or
25
26 349 preservation artifacts, they have passed unnoticed in previous investigations.

30
31 350 Pearl oysters and relatives (Pterioidea) are another pteriomorphian lineage
32
33 351 provided with numerous tentacles on both middle and inner mantle folds, also with
34
35 352 variation in size and pigmentation (Tëmkin, 2006). Our data for the pteriids *Isognomon*
36
37 353 *bicolor*, *Pinctada imbricata*, and *Pteria colymbus* are in accordance with the pattern of
38
39 354 tentacle distribution previously described for both folds, and also with the presence of
40
41 355 branched IFT in the latter two genera (Tëmkin, 2006). Interestingly, our results for
42
43 356 *Ostrea equestris* revealed great similarity to Pteriidae in respect to the increase of IFT
44
45 357 size and abundance towards the ventral region (**incurrent** aperture), as also observed in
46
47 358 *Crassostrea* spp. (Amaral & Simone, 2014). In contrast to pteriids, however, MFT are
48
49 359 submarginal in *Crassostrea* and *Ostrea*, with proximal (long) and distal (short) tentacles
50
51 360 (Amaral & Simone, 2014; present study).

52
53
54
55
56
57 361

1
2
3
4 362 *Tentacle functions and anatomical patterns*
5

6 363 The increase of tentacular size towards the **incurrent** and **excurrent** regions is a
7
8 364 common trend for many bivalve groups, especially for those with siphons (Sartori et al.,
9
10 365 2008). Even in bivalves with free mantle margins (i.e., devoid of siphons), the position
11
12 366 of the inner mantle fold may be muscularly adjusted to delimit and control the aperture
13
14 367 of **incurrent** and **excurrent** regions (Owen & McCrae, 1979). Tentacles at the **incurrent**
15
16 368 region are supposed to prevent the entrance of large particles into the mantle cavity,
17
18 369 especially in turbulent environments, where large particles would obstruct water flow
19
20 370 through the gills and mantle cavity. Our results show abundant musculature in the IFT,
21
22 371 regardless of their size or of the presence of lateral branches. **The musculature of IFT**
23
24 372 should allow for fine adjustments in tentacle position, possibly protecting the mantle
25
26 373 cavity apertures. In contrast to previous hypotheses on tentacles as non-specialized
27
28 374 extensions of the mantle margin (Waller, 1975), our data **are** in accordance with studies
29
30 375 on Pterioidea arguing for the structural and functional complexity of those structures
31
32 376 (Tëmkin, 2006). As described herein, elongated IFT at the **incurrent** region are observed
33
34 377 in Ostreidae, Pinnidae, and Pteriidae **(all of them currently placed within Ostreida, Fig.**
35
36 378 **7)**, as well as in most siphoned **bivalves**.
37
38
39
40
41
42

43 379 In particular cases, tentacles can also play defensive roles against potential
44
45 380 predators. For example, *Limaria hians* (former *Lima hians*, Limidae) can autotomize
46
47 381 parts of its tentacles, or even the entire organ, with subsequent release of distasteful
48
49 382 mucus to avoid predation (Gilmour, 1963, 1967). In the phylogenetically distant
50
51 383 Galeommatidae, anatomical data on *Galeomma takii* also suggest autotomy and
52
53 384 secretory activity as similar defensive mechanisms. When stimulated, papillae on the
54
55
56
57
58
59
60

1
2
3
4 385 middle fold, which almost completely cover the shell, are capable of autotomy,
5
6 386 secreting a noxious substance (Morton, 1973).

7
8
9 387 **Secretory activity appeared to be largely present in the species studied (Table 1).**

10
11 388 Our results show that secretion of mucosubstances is an important role performed by
12
13 389 MFT, including neutral (PAS-positive) and acidic polysaccharides (AB-positive) and
14
15 390 basic glycoproteins (BB-positive), secreted by subepithelial and epithelial secretory
16
17 391 cells. Similar results were obtained for other Pteriidae, with acidophilic secretory cells
18
19 392 and neutral glycoproteins secretion in the MFT of *Pinctada margaritifera* (Jabbour-
20
21 393 Zahab, Chagot, Blanc, & Grizel, 1992). The production of mucus by the tentacles **is**
22
23 394 expected to keep these organs clean through the agglutination of undesirable particles or
24
25 395 small organisms, propelling them to the mantle surface for rejection (Beninger & St-
26
27 396 Jean, 1997; Prezant, 1990). Another **piece of** evidence reinforcing this hypothesis is the
28
29 397 short, densely distributed cilia covering the surface of MFT in the studied species,
30
31 398 which display characteristics likely associated with mucociliary transportation (Sleigh,
32
33 399 1989; Sleigh, Blake, & Liron, 1988).

34
35
36
37
38
39 400 Secretory activity in MFT was also shown for *Nodipecten nodosus* (Audino et
40
41 401 al., 2015), including acidic and neutral mucosubstances very similar to those of
42
43 402 *Spondylus ictericus*. In the case of *N. nodosus*, cilia are densely distributed over the
44
45 403 tentacle surface (Audino et al., 2015). In contrast, *S. ictericus* exhibits longitudinal rows
46
47 404 of cilia along the MFT that are supposed to promote mucus propulsion, which is
48
49 405 supported by the presence of secretory droplets in adjacent areas.

50
51
52 406 Despite intense secretory activity in the inner mantle fold of many bivalve
53
54 407 species (Audino & Marian, 2018; Jabbour-Zahab et al., 1992; Richardson, Runham, &
55
56 408 Crisp, 1981), IFT show little or no evidence of secretory cells in the species investigated
57
58
59
60

1
2
3
4 409 herein. Nevertheless, our results indicate these organs should be able to propel the
5
6 410 mucus secreted proximally by the inner fold, possibly helping to lubricate the mantle
7
8 411 margin. Droplets of possible mucosubstance observed in the tentacles of *P. carnea* and
9
10 412 cilia distribution in the pteriids and in *O. equestris* support this hypothesis. Moreover,
11
12 413 ciliary rows observed in *O. equestris* and ciliary patches in the pteriids match the
13
14 414 conditions to provide mucociliary transportation of mucus rafts required for cleansing
15
16 415 and lubrication (Sleigh, 1989). Both roles are important for animals living in benthic
17
18 416 environments, especially where there is a high concentration of suspended particles and
19
20 417 debris that can cover, obstruct or damage the mantle margin.
21
22
23
24

25 418 Bivalve tentacles are also regarded as sensory organs due to putative mechano-
26
27 419 and chemoreceptors organized in ciliary receptor cells. Nevertheless, both functional
28
29 420 types can hardly be distinguished based exclusively on morphological criteria (Owen &
30
31 421 McCrae, 1979). Scallops and limids are, by far, the most investigated examples of
32
33 422 bivalves having specialized sensory MFT. In *Placopecten magellanicus* and *Nodipecten*
34
35 423 *nodosus*, ciliary tufts, supposedly acting as mechanoreceptors, are distributed on
36
37 424 papillae at the distal portion of long, exploratory tentacles (Audino et al., 2015; Moir,
38
39 425 1977). Ciliary papillae were not observed on the MFT of *Spondylus ictericus*, a
40
41 426 representative of a family phylogenetically close to Pectinidae (Pectinoidea, Fig. 7).
42
43 427 However, ciliary tufts are sparsely distributed on the surfaces of long tentacles, and they
44
45 428 are most likely related to sensory perception.
46
47
48
49

50 429 Sensory ciliated receptors are also common at the tip of siphons and on siphonal
51
52 430 tentacles, as observed in Donacidae and Tellinidae (Hodgson & Fielden, 1984; Vitonis
53
54 431 et al., 2012), and on papillae along the middle fold, as in *Mysella charcoti* (Lasaeidae)
55
56 432 (Passos, Domaneschi, & Sartori, 2005). In the present study, a dense ciliary cluster
57
58
59
60

1
2
3
4 433 associated with abundant innervation was consistently observed at the tip of MFT in
5
6 434 *Isognomon bicolor*, *Ostrea equestris*, *Pinctada imbricata*, and *Pteria colymbus*. These
7
8
9 435 results suggest the presence of putative sensory receptors at the tip of MFT as a shared
10
11 436 pattern for Ostreioidea and Pterioidea (Fig. 7). The widespread distribution of ciliary
12
13 437 clusters and ciliated cells in the studied MFT indicate tentacles are important sensory
14
15 438 organs for interacting with the surrounding environment, possibly detecting types of
16
17 439 substrate, predators, suspended particles, and other ecological cues.

18
19
20 440 Ciliated receptors were also observed at the tip of IFT in some pterioid and
21
22 441 ostreid species studied herein (Table 1), which suggests that that these putative
23
24 442 homologous structures play important sensory roles in addition to the protection of the
25
26 443 mantle cavity aperture. The extensive innervation associated with ciliated receptors
27
28 444 supports this hypothesis. However, lack of data for *Pinna carnea* and *Spondylus*
29
30 445 *ictericus* prevents further conclusions on innervation patterns. In the pterioid and ostreid
31
32 446 species studied herein, MFT and IFT innervation is characterized by a branching pattern
33
34 447 throughout the tentacle, resulting in numerous small nerves running along the organ and
35
36 448 reaching the ciliated cells (possibly sensory receptor cells). This suggests another
37
38 449 common pattern shared by Pterioidea and Ostreioidea (Fig. 7), which is distinct, for
39
40 450 example, from tentacle innervation in the pectinid *N. nodosus*, in which a single central
41
42 451 nerve emits very tiny projections to the epithelium (Audino et al., 2015).

43
44
45
46
47
48 452

49 453 **5. Conclusions**

50
51 454 Although the evolutionary origin and diversification of tentacles during
52
53 455 Pteriomorphia radiation are still speculative, our results support the homology of MFT
54
55 456 and IFT in Pterioidea and Ostreioidea, considering their larger size and abundance
56
57
58
59
60

1
2
3
4 457 ventrally, presence of ciliary clusters at the tip, and branched innervation pattern (Table
5
6 458 1). Even though information for additional taxa would be necessary to support such a
7
8
9 459 conclusion, our results are in accordance with phylogenetic hypotheses that recover the
10
11 460 sister relationship between these superfamilies (Tëmkin, 2010; Lemer et al., 2016; Fig.
12
13 461 7). In contrast, profound anatomical differences, such as tentacle innervation, cilia
14
15 462 organization, and size distribution along dorsal to ventral regions (Table 1), indicate IFT
16
17 463 and MFT are not homologous across Pteriomorphia. In addition, given that tentacle
18
19 464 diversification may be associated with similar selective pressures, as suggested by the
20
21 465 recurrent evolution of protective IFT in numerous bivalve lineages (e.g., Sartori et al.,
22
23 466 2008; Vitonis et al., 2012), evolutionary convergence should be expected when
24
25 467 exploring tentacle evolution in Pteriomorphia.

26
27
28
29 468 Just like most invertebrates, bivalves have evolved numerous types of tentacles
30
31 469 associated with diverse functions. The detailed anatomical analysis of pallial tentacles in
32
33 470 selected representatives of pteriomorphian bivalves revealed possible shared characters
34
35 471 for the clades **Pterioidea** and **Ostreoidea**, as well as the first anatomical description of
36
37 472 tentacles in Spondylidae and Pinnidae. **Sensory and protective roles are likely**
38
39 473 **performed by both MFT and IFT, as well as cleansing and lubrication by MFT.** In
40
41 474 conclusion, by applying integrative microscopy to study the structure and infer the
42
43 475 functional morphology of such diverse organs, we were able to reveal anatomical
44
45 476 elements that are essential for the understanding of homology when dealing with such
46
47 477 **superficially similar structures.**

48
49
50
51
52 478

53 54 479 **Acknowledgements**

1
2
3
4 480 The authors acknowledge funding provided by the grant 2015/09519-4, São
5
6 481 Paulo Research Foundation (FAPESP). This study was financed in part by the
7
8 482 Coordenação de Aperfeiçoamento de Pessoal de Nível Superior - Brasil (CAPES) -
9
10 483 Finance Code 001. This study is part of the first author's Doctorate's thesis through the
11
12 484 Graduate Program in Zoology of the Institute of Biosciences (University of São Paulo).
13
14 485 The authors thank the research grant provided by Malacological Society of London for
15
16 486 acquisition of confocal microscopy reagents. The authors thank the Center for Marine
17
18 487 Biology (CEBIMar-USP), their technical staff, and Prof. Alvaro Migotto for the
19
20 488 invaluable support in the collection and analysis of live specimens used in this study.
21
22 489 The authors also thank the Laboratory of Cell Biology (IB-USP) for providing the
23
24 490 facilities for confocal microscopy analysis and technical assistance. This is a
25
26 491 contribution of NP-BioMar (Research Center for Marine Biodiversity – USP). **The**
27
28 492 **authors also acknowledge two anonymous reviewers for helpful comments and**
29
30 493 **suggestions.**
31
32
33
34
35
36
37
38

495 **References**

- 496 Allen, J. A. (2004). The Recent species of the genera *Limatula* and *Limea* (Bivalvia,
497 Limacea) present in the Atlantic, with particular reference to those in deep water.
498 *Journal of Natural History*, 38, 2591–2653.
499 <https://doi.org/10.1080/00222930310001647442>
- 500 Amaral, V. S. D., & Simone, L. R. L. (2014). Revision of genus *Crassostrea* (Bivalvia:
501 Ostreidae) of Brazil. *Journal of the Marine Biological Association of the United*
502 *Kingdom*, 94, 811–836. <https://doi.org/10.1017/S0025315414000058>
- 503 Audino, J. A., & Marian, J. E. A. R. (2018). Comparative and functional anatomy of the
504 mantle margin in ark clams and their relatives (Bivalvia: Arcoidea) supports association
505 between morphology and life habits. *Journal of Zoology*, 305, 149–162.

- 1
2
3
4 506 <https://doi.org/10.1111/jzo.12544>
5
6
7 507 Audino, J. A., Marian, J. E. A. R., Wanninger, A., & Lopes, S. G. B. C. (2015).
8
9 508 Anatomy of the pallial tentacular organs of the scallop *Nodipecten nodosus* (Linnaeus,
10
11 509 1758) (Bivalvia: Pectinidae). *Zoologischer Anzeiger - A Journal of Comparative*
12 510 *Zoology*, 258, 39–46. <https://doi.org/10.1016/j.jcz.2015.06.004>
13
14 511 Bancroft, J., & Stevens, A. (1982). *Theory and Practice of Histological Techniques*.
15 512 New York, NY: Churchill Livingstone.
16
17
18 513 Behmer, O. A., Tolosa, E. M. C., & Freitas Neto, A. G. (1976). *Manual de técnicas*
19 514 *para microscopia normal e patológica*. São Paulo: Edusp.
20
21
22 515 Beninger, P. G., & St-Jean, S. D. (1997). The role of mucus in particle processing by
23 516 suspension-feeding marine bivalves: unifying principles. *Marine Biology*, 129, 389–
24 517 397. <https://doi.org/10.1007/s002270050179>
25
26
27 518 Bickell-Page, L. R., & Mackie, G. O. (1991). Tentacle autotomy in the hydromedusa
28 519 *Aglantha digitale* (Cnidaria): an ultrastructural and neurophysiological analysis.
29 520 *Philosophical Transactions of the Royal Society of London. Series B: Biological*
30 521 *Sciences*, 331, 155–170. <https://doi.org/10.1098/rstb.1991.0005>
31
32
33 522 Brusca, R. C., Moore, W., & Shuster, R. M. (2016). *Invertebrates* (3rd ed.). Sunderland,
34 523 MA: Sinauer Associates.
35
36
37 524 Cameron, J. L., & Fankboner, P. V. (1984). Tentacle structure and feeding processes in
38 525 life stages of the commercial sea cucumber *Parastichopus californicus* (Stimpson).
39 526 *Journal of Experimental Marine Biology and Ecology*, 81, 193–209.
40
41
42 527 [https://doi.org/10.1016/0022-0981\(84\)90006-6](https://doi.org/10.1016/0022-0981(84)90006-6)
43
44
45 528 Carter, J. G., Harries, P. J., Malchus, N., Sartori, A. F., Anderson, L. C., Bieler R, ...&
46 529 Zieritz, A. (2012). Illustrated Glossary of the Bivalvia. *Treatise Online*, 48,1–209.
47
48
49 530 <https://doi.org/10.17161/to.v0i0.4322>
50
51
52 531 Croll, R. P. (1983). Gastropod chemoreception. *Biological Reviews*, 58, 293–319.
53
54
55 532 <https://doi.org/10.1111/j.1469-185X.1983.tb00391.x>
56
57
58 533 Dakin, W. J. (1909). *Pecten*. London: Williams & Norgate.
59
60

- 1
2
3
4 534 Dakin, W. J. (1928a). The anatomy and phylogeny of *Spondylus*, with a particular
5 535 reference to the lamellibranch nervous system. *Proceedings of the Royal Society B:*
6 536 *Biological Sciences*, 103, 337–354. <https://doi.org/10.1098/rspb.1928.0046>
7
8
9
10 537 Dakin, W. J. (1928b). The eyes of *Pecten*, *Spondylus*, *Amussium* and allied
11 538 lamellibranchs, with a short discussion on their evolution. *Proceedings of the Royal*
12 539 *Society B: Biological Sciences*, 103, 355–365. <https://doi.org/10.1098/rspb.1928.0047>
13
14
15 540 Drew, G. A. (1906). *The habits anatomy, and embryology of the giant scallop. (Pecten*
16 541 *tenuicostatus, Mighels)*. Orono: University of Maine Studies.
17
18
19 542 Dubois, S., Barillé, L., Cognie, B., & Beninger, P. (2005). Particle capture and
20 543 processing mechanisms in *Sabellaria alveolata* (Polychaeta: Sabellariidae). *Marine*
21 544 *Ecology Progress Series*, 301, 159–171. <https://doi.org/10.3354/meps301159>
22
23
24 545 Fishelson, L. (2000). Comparative morphology and cytology of siphons and siphonal
25 546 sensory organs in selected bivalve molluscs. *Marine Biology*, 137, 497–509.
26
27
28 547 <https://doi.org/10.1007/s002270000354>
29
30
31 548 Gilmour, T. H. J. (1963). A note on the tentacles of *Lima hians* (Gmelin)(Bivalvia).
32 549 *Journal of Molluscan Studies*, 35, 82–85.
33
34
35 550 <https://doi.org/10.1093/oxfordjournals.mollus.a064904>
36
37
38 551 Gilmour, T. H. J. (1967). The defensive adaptations of *Lima hians* (Mollusca, Bivalvia).
39 552 *Journal of the Marine Biological Association of the United Kingdom*, 47, 209–221.
40
41
42 553 <https://doi.org/10.1017/S0025315400033671>
43
44 554 Goldberg, W. M., Grange, K. R., Taylor, G. T., & Zuniga, A. L. (1990). The structure
45 555 of sweeper tentacles in the black coral *Antipathes fiordensis*. *The Biological Bulletin*,
46 556 179, 96–104. <https://doi.org/10.2307/1541743>
47
48
49 557 Hodgson, A. N., & Fielden, L. J. (1984). The structure and distribution of peripheral
50 558 ciliated receptors in the bivalve molluscs *Donax serra* and *D. sordidus*. *Journal of*
51 559 *Molluscan Studies*, 50, 104–112. <https://doi.org/10.1093/oxfordjournals.mollus.a065848>
52
53
54 560 Humason, G. L. (1962). *Animal tissue techniques*. San Francisco & London: W. H.
55 561 Freeman and Company.
56
57
58
59
60

- 1
2
3
4 562 Jabbour-Zahab, R., Chagot, D., Blanc, F., & Grizel, H. (1992). Mantle histology,
5 563 histochemistry and ultrastructure of the pearl oyster *Pinctada margaritifera* (L.).
6 564 *Aquatic Living Resources*, 5, 287–298. <https://doi.org/10.1051/alr:1992027>
7
8
9
10 565 Junqueira, L. C. U. (1995). Histology revisited. Technical improvement promoted by
11 566 the use of hydrophilic resin embedding. *Ciência e Cultura (Journal of the Brazilian*
12 567 *Association for the Advancement of Science)*, 47, 92–95.
13
14
15 568 Künz, E., & Haszprunar, G. (2001). Comparative ultrastructure of gastropod cephalic
16 569 tentacles: Patellogastropoda, Neritaemorphi and Vetigastropoda. *Zoologischer Anzeiger*
17 570 *- A Journal of Comparative Zoology*, 240, 137–165.
18
19 571 <https://doi.org/10.1078/0044-5231-00017>
20
21
22
23 572 Lemer, S., González, V. L., Bieler, R., & Giribet, G. (2016). Cementing mussels to
24 573 oysters in the pteriomorphian tree: a phylogenomic approach. *Proceedings of the Royal*
25 574 *Society B: Biological Sciences*, 283(1833), 20160857.
26
27 575 <https://doi.org/10.1098/rspb.2016.0857>
28
29
30
31 576 Machado, F. M., Morton, B., & Passos, F. D. (2017). Functional morphology of
32 577 *Cardiomya cleryana* (d'Orbigny, 1842) (Bivalvia: Anomalodesmata: Cuspidariidae)
33 578 from Brazilian waters: new insights into the lifestyle of carnivorous bivalves. *Journal of*
34 579 *the Marine Biological Association of the United Kingdom*, 97, 447–462.
35
36 580 <https://doi.org/10.1017/S0025315416000564>
37
38
39
40
41 581 Mikkelsen, P. M., & Bieler, R. (2003). Systematic revision of the western Atlantic file
42 582 clams, *Lima* and *Ctenoides* (Bivalvia: Limoida: Limidae). *Invertebrate Systematics*, 17,
43 583 667. <https://doi.org/10.1071/IS03007>
44
45
46
47 584 Moir, A. J. G. (1977). Ultrastructural studies on the ciliated receptors of the long
48 585 tentacles of the giant scallop, *Placopecten magellanicus* (Gmelin). *Cell and Tissue*
49 586 *Research*, 184, 367–380. <https://doi.org/10.1007/BF00219897>
50
51
52
53 587 Morton, B. (1973). The biology and functional morphology of *Galeomma* (Paralepida)
54 588 *takii* (Bivalvia: Leptonacea). *Journal of Zoology*, 169, 133–150.
55
56 589 <https://doi.org/10.1111/j.1469-7998.1973.tb04549.x>
57
58
59
60

- 1
2
3
4 590 Narchi, W. (1972). Comparative study of the functional morphology of *Anomalocardia*
5 591 *brasiliiana* (Gmelin, 1791) and *Tivela mactroides* (Born, 1778)(Bivalvia, Veneridae).
6 592 *Bulletin of Marine Science*, 22, 643–670.
- 7
8
9
10 593 Nielsen, C., & Riisgård, H. (1998). Tentacle structure and filter-feeding in *Crisia*
11 594 *eburnea* and other cyclostomatous bryozoans, with a review of upstream-collecting
12 595 mechanisms. *Marine Ecology Progress Series*, 168, 163–186.
13
14
15 596 <https://doi.org/doi:10.3354/meps168163>
- 16
17
18 597 Owen, G., & McCrae, J. M. (1979). Sensory cell/gland cell complexes associated with
19 598 the pallial tentacles of the bivalve *Lima hians* (Gmelin), with a note on specialized cilia
20 599 on the pallial curtains. *Philosophical Transactions of the Royal Society B: Biological*
21 600 *Sciences*, 287, 45–62. <https://doi.org/10.1098/rstb.1979.0052>
- 22
23
24
25 601 Passos, F. D., Domaneschi, O., & Sartori, A. F. (2005). Biology and functional
26 602 morphology of the pallial organs of the Antarctic bivalve *Mysella charcoti* (Lamy,
27 603 1906) (Galeommatoidea: Lasaeidae). *Polar Biology*, 28, 372–380.
28
29
30 604 <https://doi.org/10.1007/s00300-004-0702-5>
- 31
32
33 605 Passos, F. D., & Machado, F. M. (2014). A new species of *Cyamiocardium* Soot-Ryen,
34 606 1951 from shallow waters off Brazil, with a discussion on the anatomical characters of
35 607 the cyamiidae (Bivalvia: Cyamioidea). *American Malacological Bulletin*, 32, 122–131.
36
37
38 608 <https://doi.org/10.4003/006.032.0110>
- 39
40
41 609 Pearse, A. G. E. (1985). *Histochemistry, theoretical and applied* (4th ed., Vol. 2).
42 610 London: Churchill Livingstone.
- 43
44
45 611 Piffer, P. R., Arruda, E. P. de, & Passos, F. D. (2011). The biology and functional
46 612 morphology of *Macoma biota* (Bivalvia: Tellinidae: Macominae). *Zoologia (Curitiba,*
47 613 *Impresso)*, 28, 321–333. <http://dx.doi.org/10.1590/S1984-46702011000300006>
- 48
49
50 614 Pilger, J. F. (1982). Ultrastructure of the tentacles of *Themiste lageniformis* (Sipuncula).
51 615 *Zoomorphology*, 100, 143–156. <https://doi.org/10.1007/BF0031036>
- 52
53
54 616 Prezant, R. S. (1990). Form, function and phylogeny of bivalve mucins. In *The*
55 617 *Bivalvia—The Proceedings of a Memorial Symposium in Honour of Sir Charles*
56 618 *Maurice Yonge* (pp. 83–95). Hong Kong: Hong Kong University Press.
- 57
58
59
60

- 1
2
3
4 619 Richardson, C. A., Runham, N. W., & Crisp, D. J. (1981). A histological and
5
6 620 ultrastructural study of the cells of the mantle edge of a marine bivalve, *Cerastoderma*
7
8 621 *edule*. *Tissue and Cell*, 13, 715–730. [https://doi.org/10.1016/S0040-8166\(81\)80008-0](https://doi.org/10.1016/S0040-8166(81)80008-0)
9
10 622 Rifkin, J. F. (1991). A study of the spirocytes from the Ceriantharia and Actiniaria
11
12 623 (Cnidaria: Anthozoa). *Cell and Tissue Research*, 266, 365–373.
13
14 624 <https://doi.org/10.1007/BF00318192>
15
16 625 Riisgård, H. U. (2002). Methods of ciliary filter feeding in adult *Phoronis muelleri*
17
18 626 (phylum Phoronida) and in its free-swimming actinotroch larva. *Marine Biology*, 141,
19
20 627 75–87. <https://doi.org/10.1007/s00227-002-0802-0>
21
22 628 Roberts, D., & Moore, H. M. (1997). Tentacular diversity in deep-sea deposit-feeding
23
24 629 holothurians: implications for biodiversity in the deep sea. *Biodiversity & Conservation*,
25
26 630 6(11), 1487–1505. <https://doi.org/10.1023/A:1018362319053>
27
28 631 Sartori, André F, & Domaneschi, O. (2005). The functional morphology of the antarctic
29
30 632 bivalve *Thracia meridionalis* Smith, 1885 (Anomalodesmata: Thraciidae). *Journal of*
31
32 633 *Molluscan Studies*, 71, 199–210. <https://doi.org/10.1093/mollus/eyi028>
33
34 634 Sartori, André Fernando, Printrakoon, C., Mikkelsen, P. M., & Bieler, R. (2008).
35
36 635 Siphonal structure in the Veneridae (Bivalvia: Heterodonta) with an assessment of its
37
38 636 phylogenetic application and a review of venerids of the Gulf of Thailand. *The Raffles*
39
40 637 *Bulletin of Zoology*, 18, 103–125.
41
42 638 Shimizu, H., & Namikawa, H. (2009). The body plan of the cnidarian medusa: distinct
43
44 639 differences in positional origins of polyp tentacles and medusa tentacles. *Evolution &*
45
46 640 *Development*, 11, 619–621. <https://doi.org/10.1111/j.1525-142X.2009.00368.x>
47
48 641 Sleight, M. A. (1989). Adaptations of ciliary systems for the propulsion of water and
49
50 642 mucus. *Comparative Biochemistry and Physiology Part A: Physiology*, 94, 359–364.
51
52 643 [https://doi.org/10.1016/0300-9629\(89\)90559-8](https://doi.org/10.1016/0300-9629(89)90559-8)
53
54 644 Sleight, M. A., Blake, J. R., & Liron, N. (1988). The propulsion of mucus by cilia.
55
56 645 *American Review of Respiratory Disease*, 137, 726–741.
57
58 646 <https://doi.org/10.1164/ajrccm/137.3.726>
59
60

- 1
2
3
4 647 Tamberg, Y., & Shunatova, N. (2016). Feeding behavior in freshwater bryozoans:
5 648 function, form, and flow. *Invertebrate Biology*, 135, 138–149.
6
7
8 649 <https://doi.org/10.1111/ivb.12124>
9
10 650 Tamberg, Y., & Shunatova, N. (2017). Tentacle structure in freshwater bryozoans.
11 651 *Journal of Morphology*, 278, 718–733. <https://doi.org/10.1002/jmor.20666>
12
13
14 652 Tëmkin, I. (2006). Morphological perspective on the classification and evolution of
15 653 Recent Pterioidea (Mollusca: Bivalvia). *Zoological Journal of the Linnean Society*, 148,
16 654 253–312. <https://doi.org/10.1111/j.1096-3642.2006.00257.x>
17
18
19 655 Thorington, G. U., & Hessinger, D. A. (1998). Efferent mechanisms of discharging
20 656 cnidae: II. A nematocyst release response in the sea anemone tentacle. *The Biological*
21 657 *Bulletin*, 195, 145–155. <https://doi.org/10.2307/1542822>
22
23
24 658 Vitonis, J. E. V. V., Zaniratto, C. P., Machado, F. M., & Passos, F. D. (2012).
25 659 Comparative studies on the histology and ultrastructure of the siphons of two species of
26 660 Tellinidae (Mollusca: Bivalvia) from Brazil. *Zoologia (Curitiba)*, 29, 219–226.
27 661 <https://doi.org/10.1590/S1984-46702012000300005>
28
29
30 662 von Byern, J., Wani, R., Schwaha, T., Grunwald, I., & Cyran, N. (2012). Old and
31 663 sticky—adhesive mechanisms in the living fossil *Nautilus pompilius* (Mollusca,
32 664 Cephalopoda). *Zoology*, 115, 1–11. <https://doi.org/10.1016/j.zool.2011.08.002>
33
34
35 665 Waller, T. R. (1975). The behavior and tentacle morphology of pteriomorphian
36 666 bivalves: a motion-picture study. *Bulletin of the American Malacological Union*, 7–13.
37
38
39 667 Watson, G. M., & Mariscal, R. N. (1983). The development of a sea anemone tentacle
40 668 specialized for aggression: morphogenesis and regression of the catch tentacle of
41 669 *Haliplanella luciae* (Cnidaria, Anthozoa). *The Biological Bulletin*, 164, 506–517.
42
43
44 670 <https://doi.org/10.2307/1541259>
45
46
47 671 Yonge, C. M. (1953). Form and habit in *Pinna carnea* Gmelin. *Philosophical*
48 672 *Transactions of the Royal Society B: Biological Sciences*, 237, 335–374.
49
50
51 673 <https://doi.org/10.1098/rstb.1953.0006>
52
53
54
55
56
57
58
59
60

- 1
2
3
4 674 Yonge, C. M. (1983). Symmetries and the role of the mantle margins in the bivalve
5
6 675 Mollusca. *Malacological Review*, 16, 1–10.
7
8 676 Zhadan, A. E., & Tzetlin, A. B. (2002). Comparative morphology of the feeding
9
10 677 apparatus in the Terebellida (Annelida: Polychaeta). *Cahiers de Biologie Marine*, 43(2),
11
12 678 149–164.
13
14 679

15
16
17
18
19
20
21
22
23
24
25
26
27
28
29
30
31
32
33
34
35
36
37
38
39
40
41
42
43
44
45
46
47
48
49
50
51
52
53
54
55
56
57
58
59
60

For Peer Review

680 **Figure Legends**

681

682 **Figure 1.** Mantle tentacles of *Pteria colymbus* (Pteriidae). Middle fold tentacles (MFT)
683 in (b-g) and inner fold tentacles (IFT) in (h-l). (a). MFT (black arrows) and IFT (white
684 arrows) in the posterodorsal region. (b). **Longitudinal** section of a tentacle showing
685 subepithelial secretory cells with granular content (arrowheads); HE. (c). Same as (b),
686 but stained with BB, evidencing protein aggregates (arrowheads). (d). Same as (b), but
687 stained with AB, evidencing acidic mucosubstances (arrowheads). (e). Ciliary tufts
688 covering the tentacle surface at its base; scanning electron micrograph (SEM). (f). Cilia
689 cluster at the tip of the tentacle; SEM. (g). Tentacle musculature with abundant
690 longitudinal fibers; confocal micrograph (CLSM). (h). Tentacles on the inner fold; some
691 of them are branched (white arrows), ventral region. (i). Dense cilia distribution on
692 short, not-branched tentacles; SEM. (j). Branched tentacle with typical flattened shape;
693 SEM. (k). Detail from the previous image, showing cilia distribution; SEM. (l).
694 Musculature in a branched tentacle, including branching fibers; CLSM.

695
696 **Figure 2.** Mantle tentacles of *Pinctada imbricata* (Pteriidae). Middle fold tentacles in
697 (a-c) and inner fold tentacles in (d-h). (a). **Longitudinal** section showing subepithelial
698 secretory cells with acidic mucosubstances (arrowheads); AB. (b). **Ciliary** cluster at the
699 tip of the tentacle; scanning electron micrograph (SEM). (c). Muscle fibers (yellow)
700 along the tentacle, nuclei in blue; confocal micrograph (CLSM). (d). Branched tentacles
701 **in** the ventral region. (e). **Longitudinal** section of the tentacle, showing the absence of
702 secretory content; PAS. (f). Branched tentacle with sparse tufts of cilia; SEM. (g).
703 Detail of the epithelium of a branched tentacle; SEM. (h). Branched tentacle innervation

1
2
3
4 704 (in green) with branching nerves reaching the ciliary rootlets at the tips of the branches;
5
6 705 nuclei in blue; CLSM.

7
8
9 706

10
11 707 **Figure 3.** Mantle tentacles of *Isognomon bicolor* (Pteriidae). Middle fold tentacles in
12
13 708 (a-f) and inner fold tentacles in (g-h). (a). Longitudinal section showing subepithelial
14
15 709 secretory cells with granular content (arrowheads); HE. (b). Same as (a), but showing
16
17 710 subepithelial secretory cells with granular content stained in light blue (arrowhead), and
18
19 711 epithelial secretory cells stained in pink (arrows); TF. (c). Longitudinal section showing
20
21 712 epithelial secretory cells with acidic mucosubstances (arrowheads); AB. (d). Cilia
22
23 713 distribution on the tentacle; scanning electron micrograph (SEM). Ciliary tufts are
24
25 714 largely scarce on the inner surface. (e). Detail of the ciliary cluster at the tip of the
26
27 715 tentacle; SEM. (f). Tentacle musculature with prominent longitudinal fibers; confocal
28
29 716 micrograph (CLSM). (g). Cilia distribution on tentacle surface; SEM. (h). Cilia
30
31 717 distribution (in green), including long rootlets possibly related to innervation; nuclei in
32
33 718 blue; CLSM.

34
35
36
37
38
39 719

40
41 720 **Figure 4.** Mantle tentacles of *Ostrea equestris* (Ostreidae). Middle fold tentacles in (a-f)
42
43 721 and inner fold tentacles in (g-k). (a). Longitudinal section showing two types of
44
45 722 subepithelial secretory cells, which either have more densely (white arrowheads) or
46
47 723 more sparsely distributed granules (black arrowheads); TF. (b). Same as (a), but stained
48
49 724 with HE, showing the eosinophilic nature of the secretory cells with more densely
50
51 725 distributed granules (white arrowheads). (c). Same as (a), but stained with BB,
52
53 726 evidencing the proteinaceous content of the secretory cell type with sparsely distributed
54
55 727 granules (black arrowheads). (d). Cilia distribution on the distal portion of the tentacle;
56
57
58
59
60

1
2
3
4 728 scanning electron micrograph (SEM). (e). Mantle and tentacle musculature; confocal
5
6 729 micrograph (CLSM). (f). Branching nerves (in green) reaching the ciliary rootlets from
7
8 730 the **ciliary** cluster at the tip of the tentacle; nuclei in blue; CLSM. (g). **Longitudinal**
9
10 731 section of the mantle margin, showing an enlarged, marginal inner fold tentacle (te)
11
12 732 with no evidence of secretory cells; HE. (h). Cilia distribution on the distal portion of
13
14 733 the tentacle; SEM. (i). Detail of (h), showing ciliary tufts; SEM. (j). Detail of the cilia
15
16 734 cluster at the tip; SEM. (k). Tentacle musculature; CLSM.
17
18
19
20
21
22

23 736 **Figure 5.** Inner fold tentacles of *Pinna carnea* (Pinnidae). (a). Posterior view of the
24
25 737 tentacles located on the margin of the inner mantle fold at the **incurrent** region. (b).
26
27 738 Uniform **ciliary** distribution on the tentacle; scanning electron micrograph (SEM). (c).
28
29 739 Detail of cilia and droplets of possible mucosubstances (arrowheads); SEM. (d).
30
31 740 Tentacle musculature with longitudinal fibers greatly contracted; confocal micrograph.
32
33
34
35

36 742 **Figure 6.** Mantle tentacles of *Spondylus ictericus* (Spondylidae). Middle fold tentacles
37
38 743 (MFT) in (b-f) and inner fold tentacles (IFT) in (g-i). Scanning electron micrographs in
39
40 744 (d-h). (a). Tentacle types on the mantle margin: MFT (black arrows), including very
41
42 745 long tentacles (arrowhead), and very small IFT (white arrows; inset). (b). **Longitudinal**
43
44 746 section of the mantle margin, showing tentacles formed on the inner surface of the
45
46 747 middle fold; HE. (c). Different types of epithelial secretory cells distinguished by
47
48 748 neutral (magenta) and acidic (blue) mucosubstances; AB and PAS combined method.
49
50 749 (d). Sparse tufts of cilia on the distal portion of a long tentacle. (e). Cilia organized in
51
52 750 longitudinal rows on the surface of tentacles. (f). Detail from (e), showing a droplet
53
54 751 (arrowhead) released close to the **ciliary** row, indicating possible secretion of
55
56
57
58
59
60

1
2
3
4 752 mucosubstances. (g). Small tentacles on the margin of the inner fold. (h). Ciliary tufts
5
6 753 sparsely distributed on the tentacle surface. (i). Muscle fibers of a small tentacle;
7
8
9 754 confocal micrograph. Abbreviations: if, inner mantle fold; pe, pallial eye; te, tentacles.
10
11 755

12
13 756 **Figure 7.** Schematic representation of the Pteriomorphia phylogenetics, including
14
15 757 current orders (in bold) and superfamilies. Redrawn after Lemer et al. (2016).
16
17

18 758
19
20 759 **Supplementary Figure S1.** Innervation of MFT (a, c, d) and IFT (b) in pteriomorphian
21
22 760 species. Confocal micrographs in (a-c) and histological longitudinal section in (d). (a).
23
24 761 Central tentacular nerves that branch towards the tip (*Pteria colymbus*). (b). Branching
25
26 762 tentacular nerves (*Pteria colymbus*). (c). Branching tentacular nerves (*Pinctada*
27
28 763 *imbricata*). (d) Central tentacular nerve (*Spondylus ictericus*).
29
30
31
32
33
34
35
36
37
38
39
40
41
42
43
44
45
46
47
48
49
50
51
52
53
54
55
56
57
58
59
60

Table 1. Comparative morphology of inner (IFT) and middle fold tentacles (MFT) in Pteriomorphia. “Morphology” refers to size variation among adjacent tentacles (1 – similar size or 2 – varying size) and presence of branched tentacles (3). In the ventral region of the body, tentacles can be either (1) larger and more abundant in comparison to the anterior and posterior regions, or (2) similar to the other regions. Absence of a trait is indicated by “–” and unavailable information by “?”. For additional anatomical information, please see the results described in the main text. All data generated by the present study, except those for *Limaria hians* (sources: Gilmour 1967, Owen & McCrae 1979) and *Nodipecten nodosus* (source: Audino et al. 2015).

Species	MFT						
	Position on the fold	Morphology	Ventral region	Secretory cells	Cluster of cilia at the tip	Musculature	Innervation
<i>Pteria colymbus</i>	marginal	2	1	eosin & BB; PAS & AB	present	LM, TM	BN
<i>Pinctada imbricata</i>	marginal	2	1	eosin; PAS & AB	present	LM	BN
<i>Isognomon bicolor</i>	marginal	1	1	eosin & TF (light blue); AB & TF (pink)	present	LM, TM	?
<i>Ostrea equestris</i>	submarginal	2	1	eosin & TF (light blue); BB & TF (dark blue)	present	LM, TM	BN
<i>Pinna carnea</i>	–	–	–	–	–	–	–
<i>Limaria hians</i>	submarginal	2	2	?	–	LM, TM	CN
<i>Nodipecten nodosus</i>	submarginal	2	2	PAS & AB	–	LM, TM	CN
<i>Spondylus ictericus</i>	submarginal	2	2	PAS, AB & TF (light blue)	–	LM, TM	CN
IFT							
<i>Pteria colymbus</i>	marginal	2, 3	1	–	–	LM, TM	BN
<i>Pinctada imbricata</i>	marginal	2, 3	1	–	present	LM, TM	BN
<i>Isognomon bicolor</i>	marginal	1	1	–	present	LM, TM	BN
<i>Ostrea equestris</i>	marginal	1	1	–	present	LM	BN
<i>Pinna carnea</i>	marginal	1	–	–	–	LM, TM	?
<i>Limaria hians</i>	–	–	–	–	–	–	–
<i>Nodipecten nodosus</i>	submarginal	1	2	–	–	LM, TM	CN
<i>Spondylus ictericus</i>	marginal	1	2	–	–	LM, TM	?

Abbreviations: AB, alcian blue; BB, mercury-bromophenol blue; BN, branching nerves; CN, central nerve; LM, longitudinal muscles; PAS, periodic acid-Schiff stain; TF, toluidine blue and basic fuchsin; TM, transverse muscles.

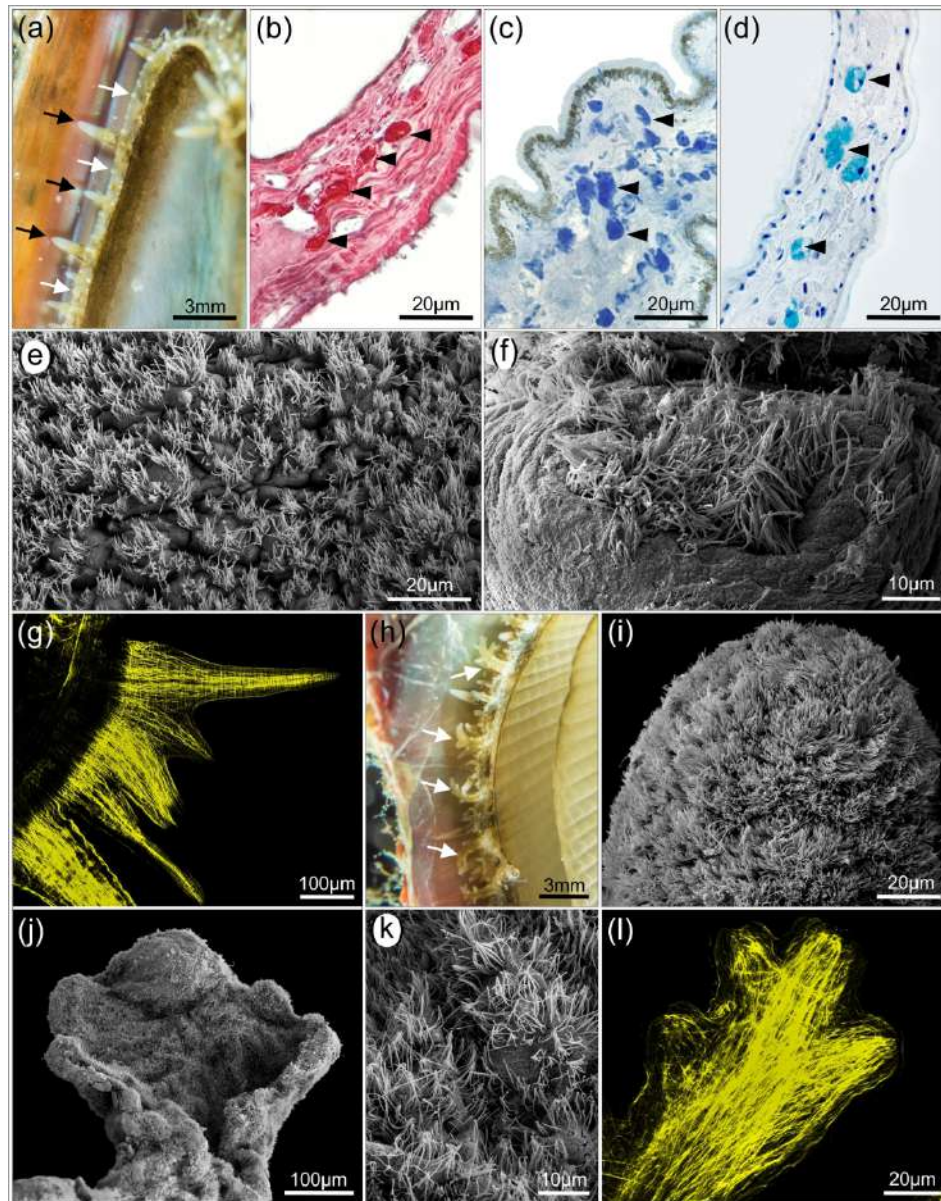
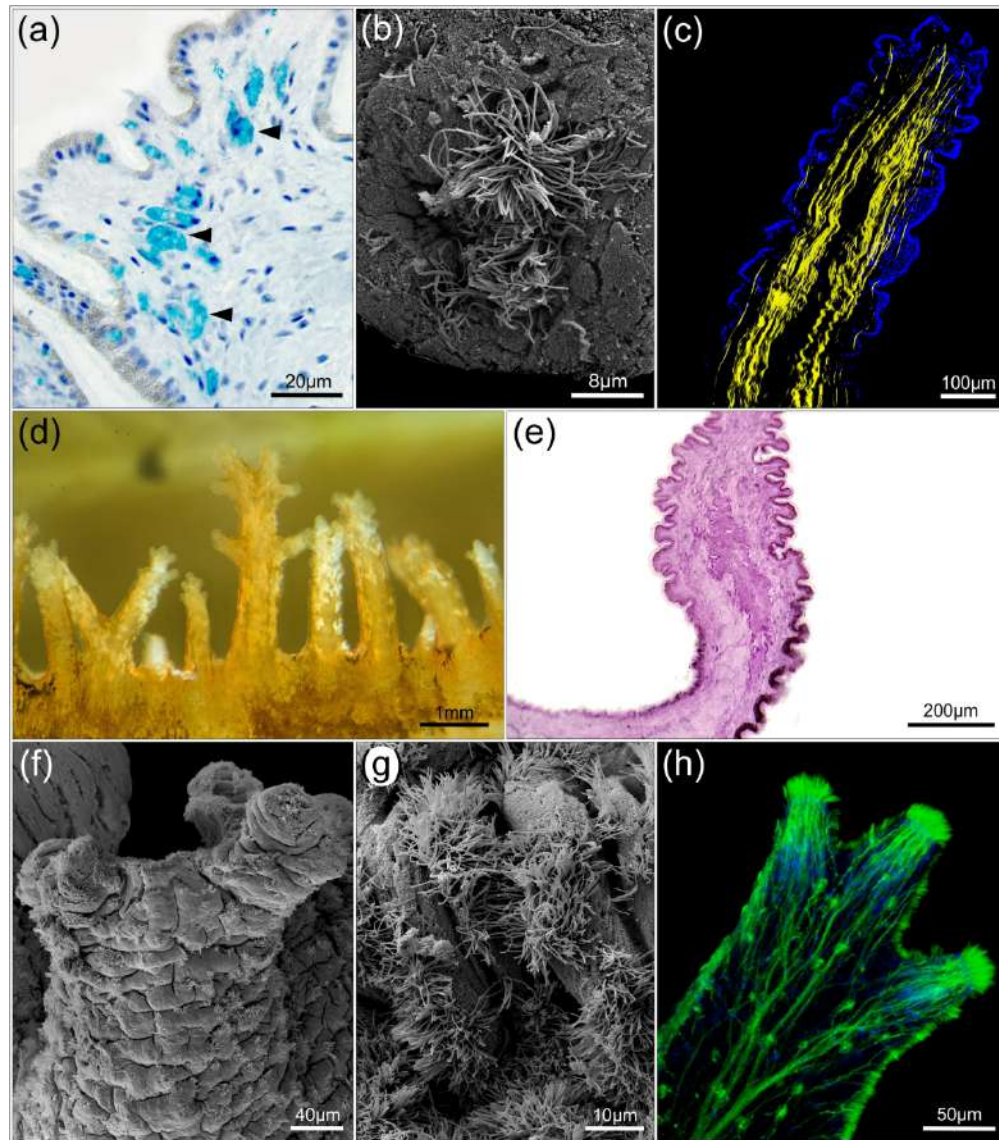
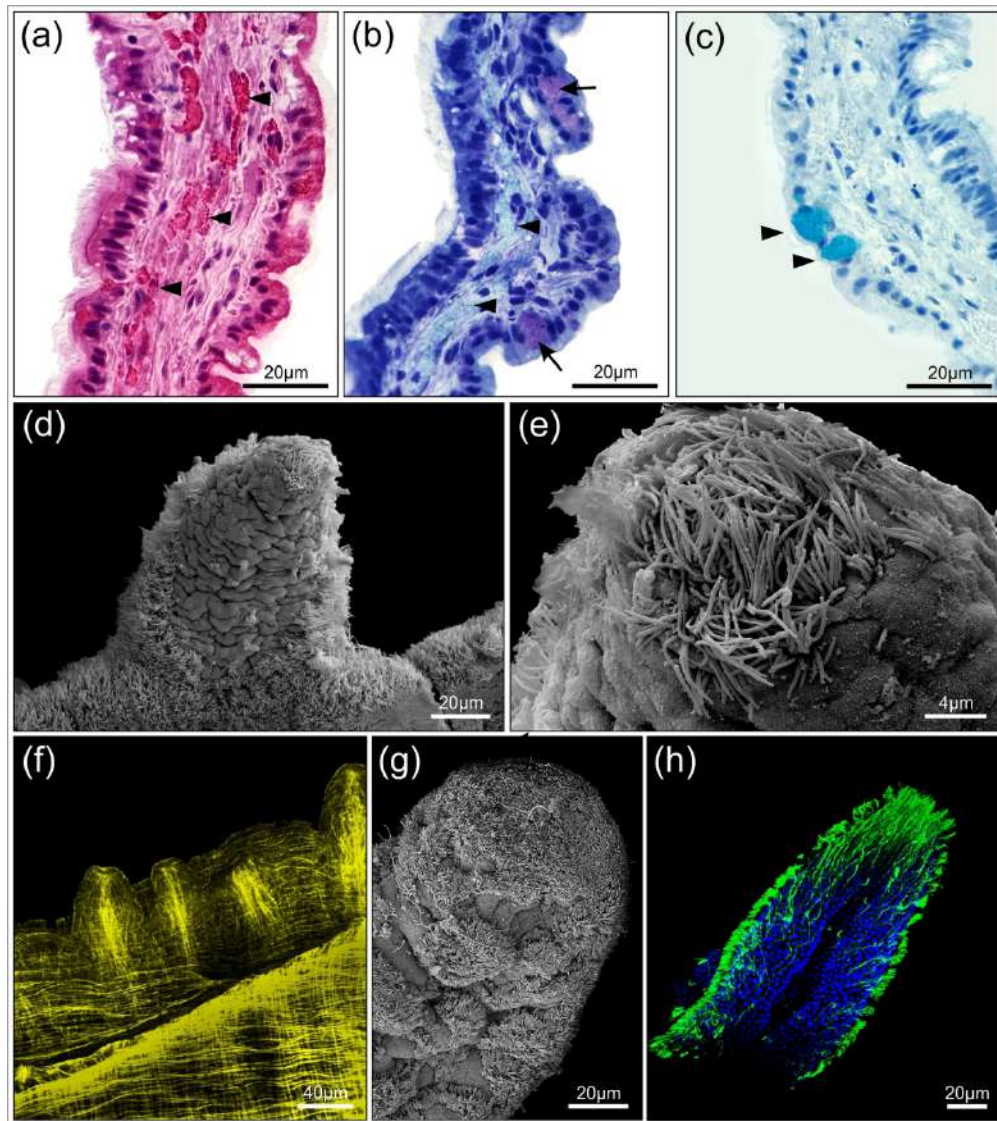


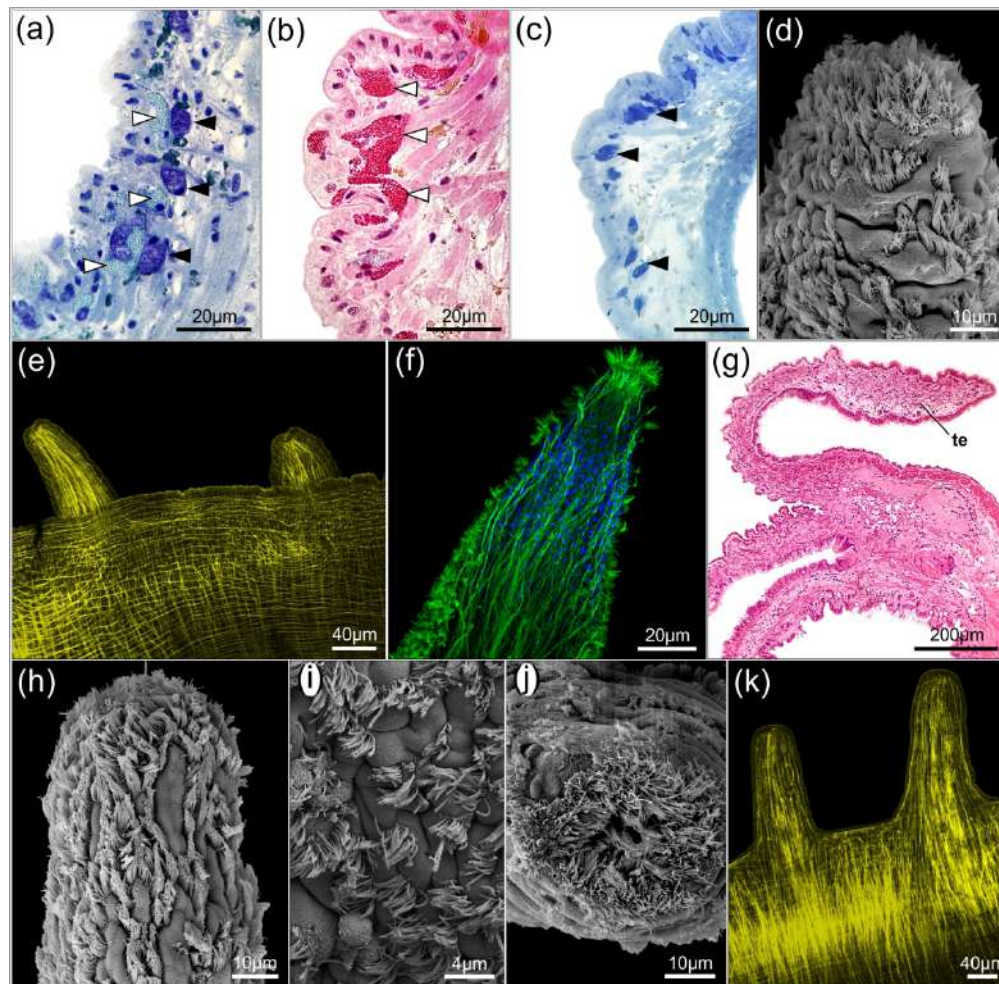
Figure 1. Mantle tentacles of *Pteria colymbus* (Pteriidae). Middle fold tentacles (MFT) in (b-g) and inner fold tentacles (IFT) in (h-l). (a). MFT (black arrows) and IFT (white arrows) in the posterodorsal region. (b). Longitudinal section of a tentacle showing subepithelial secretory cells with granular content (arrowheads); HE. (c). Same as (b), but stained with BB, evidencing protein aggregates (arrowheads). (d). Same as (b), but stained with AB, evidencing acidic mucosubstances (arrowheads). (e). Ciliary tufts covering the tentacle surface at its base; scanning electron micrograph (SEM). (f). Cilia cluster at the tip of the tentacle; SEM. (g). Tentacle musculature with abundant longitudinal fibers; confocal micrograph (CLSM). (h). Tentacles on the inner fold; some of them are branched (white arrows), ventral region. (i). Dense cilia distribution on short, not-branched tentacles; SEM. (j). Branched tentacle with typical flattened shape; SEM. (k). Detail from the previous image, showing cilia distribution; SEM. (l). Musculature in a branched tentacle, including branching fibers; CLSM.



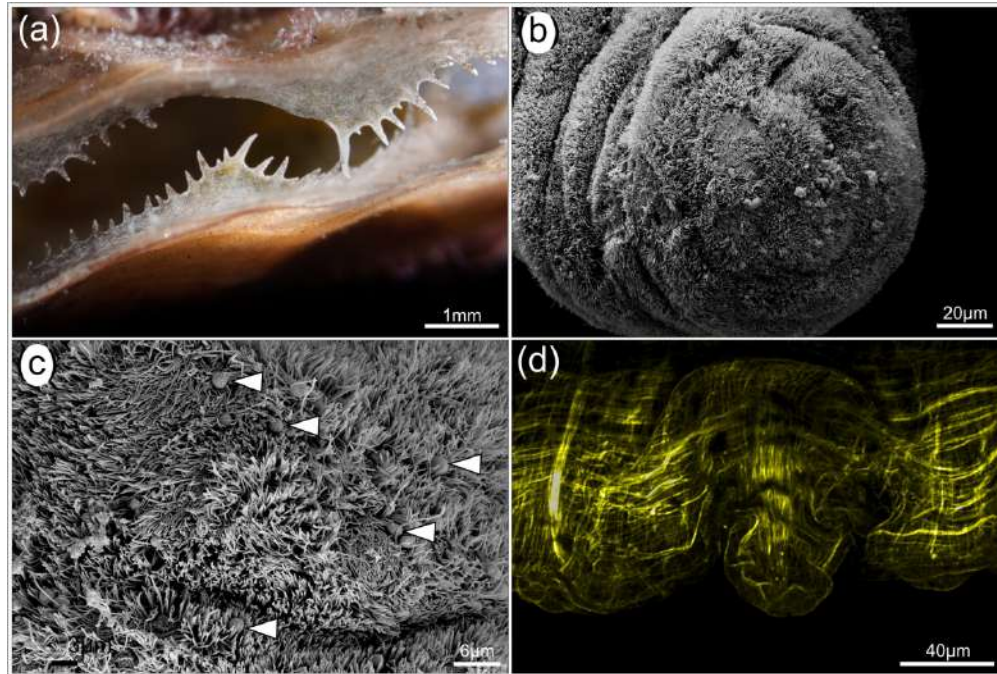
Mantle tentacles of *Pinctada imbricata* (Pteriidae). Middle fold tentacles in (a-c) and inner fold tentacles in (d-h). (a). Longitudinal section showing subepithelial secretory cells with acidic mucosubstances (arrowheads); AB. (b). Ciliary cluster at the tip of the tentacle; scanning electron micrograph (SEM). (c). Muscle fibers (yellow) along the tentacle, nuclei in blue; confocal micrograph (CLSM). (d). Branched tentacles in the ventral region. (e). Longitudinal section of the tentacle, showing the absence of secretory content; PAS. (f). Branched tentacle with sparse tufts of cilia; SEM. (g). Detail of the epithelium of a branched tentacle; SEM. (h). Branched tentacle innervation (in green) with branching nerves reaching the ciliary rootlets at the tips of the branches; nuclei in blue; CLSM.



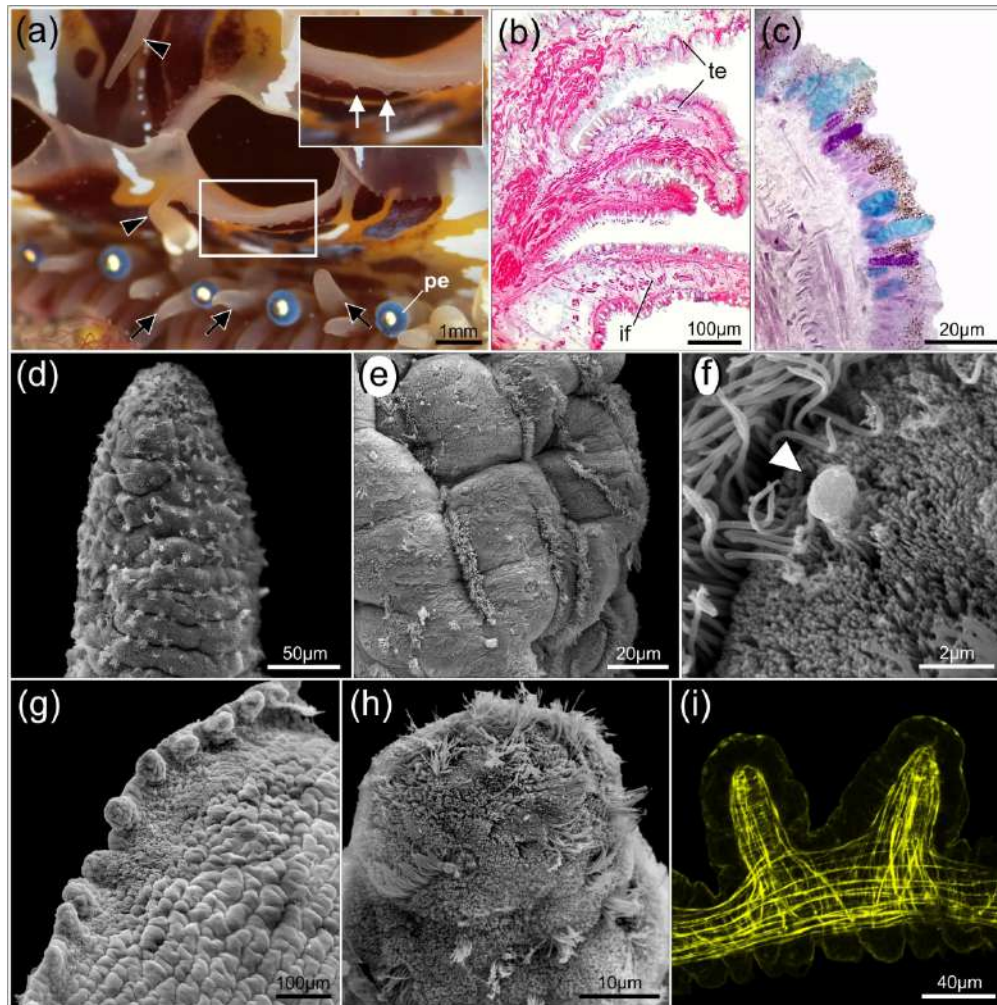
Mantle tentacles of *Isognomon bicolor* (Pteriidae). Middle fold tentacles in (a-f) and inner fold tentacles in (g-h). (a). Longitudinal section showing subepithelial secretory cells with granular content (arrowheads); HE. (b). Same as (a), but showing subepithelial secretory cells with granular content stained in light blue (arrowhead), and epithelial secretory cells stained in pink (arrows); TF. (c). Longitudinal section showing epithelial secretory cells with acidic mucosubstances (arrowheads); AB. (d). Cilia distribution on the tentacle; scanning electron micrograph (SEM). Ciliary tufts are largely scarce on the inner surface. (e). Detail of the ciliary cluster at the tip of the tentacle; SEM. (f). Tentacle musculature with prominent longitudinal fibers; confocal micrograph (CLSM). (g). Cilia distribution on tentacle surface; SEM. (h). Cilia distribution (in green), including long rootlets possibly related to innervation; nuclei in blue; CLSM.



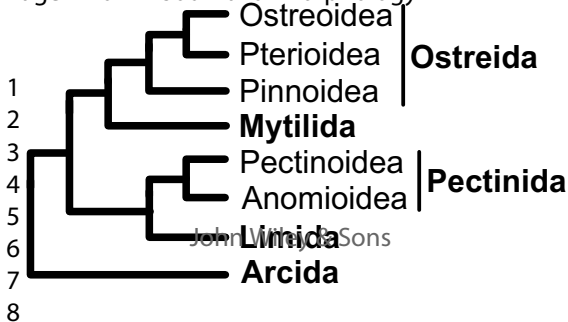
Mantle tentacles of *Ostrea equestris* (Ostreidae). Middle fold tentacles in (a-f) and inner fold tentacles in (g-k). (a). Longitudinal section showing two types of subepithelial secretory cells, which either have more densely (white arrowheads) or more sparsely distributed granules (black arrowheads); TF. (b). Same as (a), but stained with HE, showing the eosinophilic nature of the secretory cells with more densely distributed granules (white arrowheads). (c). Same as (a), but stained with BB, evidencing the proteinaceous content of the secretory cell type with sparsely distributed granules (black arrowheads). (d). Cilia distribution on the distal portion of the tentacle; scanning electron micrograph (SEM). (e). Mantle and tentacle musculature; confocal micrograph (CLSM). (f). Branching nerves (in green) reaching the ciliary rootlets from the ciliary cluster at the tip of the tentacle; nuclei in blue; CLSM. (g). Longitudinal section of the mantle margin, showing an enlarged, marginal inner fold tentacle (te) with no evidence of secretory cells; HE. (h). Cilia distribution on the distal portion of the tentacle; SEM. (i). Detail of (h), showing ciliary tufts; SEM. (j). Detail of the cilia cluster at the tip; SEM. (k). Tentacle musculature; CLSM.

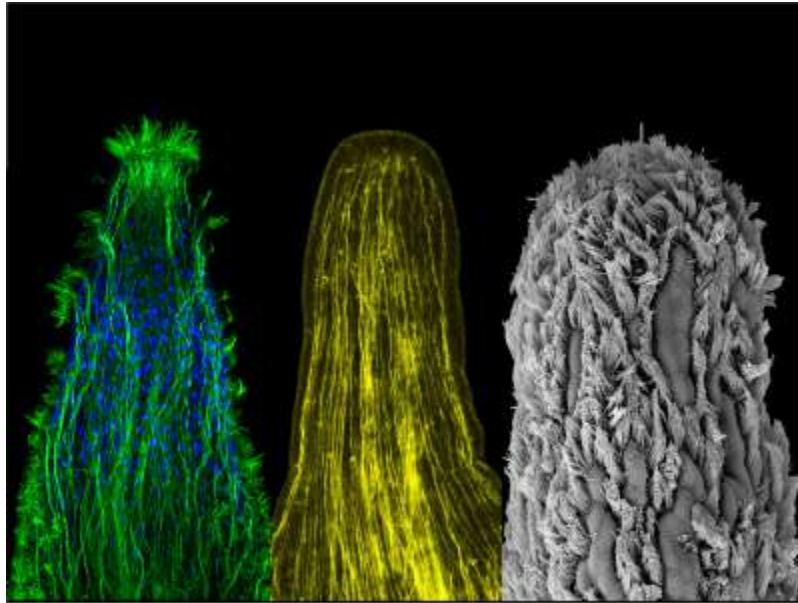


Inner fold tentacles of *Pinna carnea* (Pinnidae). (a). Posterior view of the tentacles located on the margin of the inner mantle fold at the incurrent region. (b). Uniform ciliary distribution on the tentacle; scanning electron micrograph (SEM). (c). Detail of cilia and droplets of possible mucosubstances (arrowheads); SEM. (d). Tentacle musculature with longitudinal fibers greatly contracted; confocal micrograph.



Mantle tentacles of *Spondylus ictericus* (Spondylidae). Middle fold tentacles (MFT) in (b-f) and inner fold tentacles (IFT) in (g-i). Scanning electron micrographs in (d-h). (a). Tentacle types on the mantle margin: MFT (black arrows), including very long tentacles (arrowhead), and very small IFT (white arrows; inset). (b). Longitudinal section of the mantle margin, showing tentacles formed on the inner surface of the middle fold; HE. (c). Different types of epithelial secretory cells distinguished by neutral (magenta) and acidic (blue) mucosubstances; AB and PAS combined method. (d). Sparse tufts of cilia on the distal portion of a long tentacle. (e). Cilia organized in longitudinal rows on the surface of tentacles. (f). Detail from (e), showing a droplet (arrowhead) released close to the ciliary row, indicating possible secretion of mucosubstances. (g). Small tentacles on the margin of the inner fold. (h). Ciliary tufts sparsely distributed on the tentacle surface. (i). Muscle fibers of a small tentacle; confocal micrograph. Abbreviations: if, inner mantle fold; pe, pallial eye; te, tentacles.





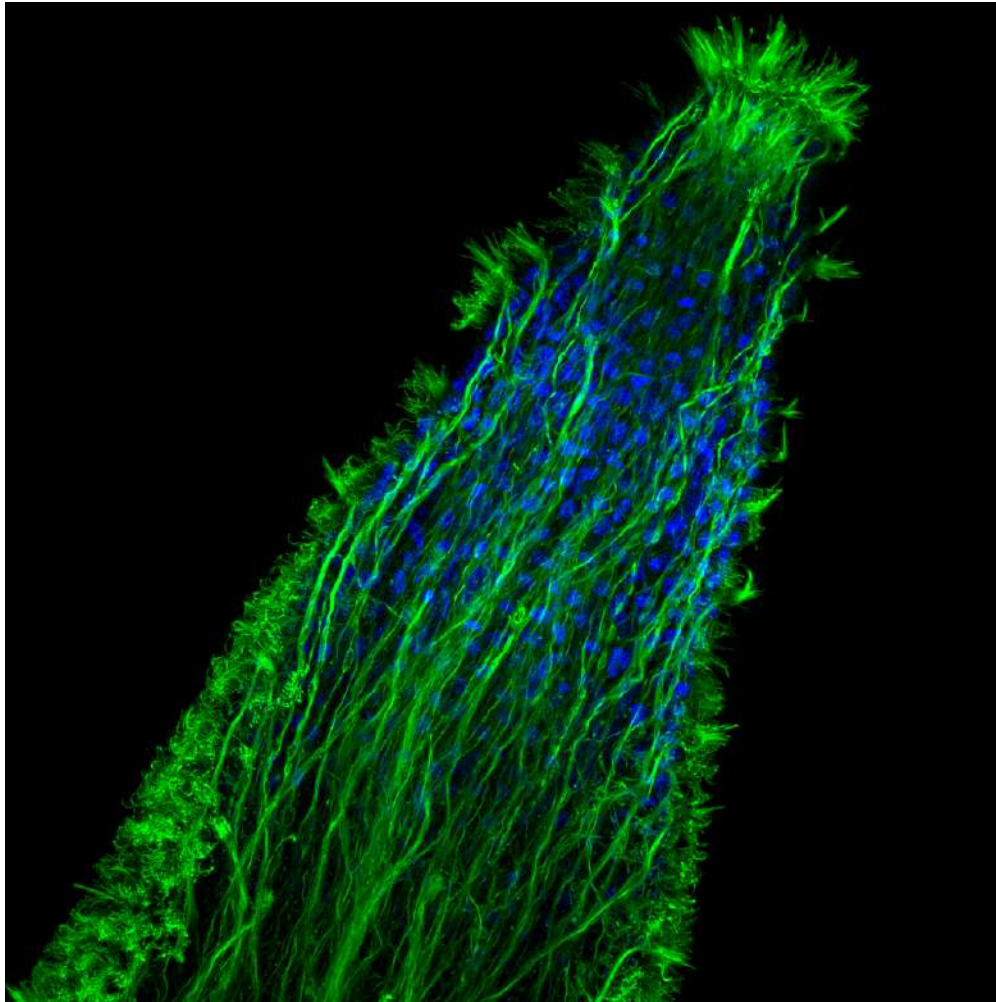
Graphical Abstract Image

Detailed microscopy analysis of mantle tentacles in pteriomorphian bivalves not only provided anatomical evidence to infer the functional morphology of such diverse organs, including sensory roles, mucociliary transportation, and protective functions, but also revealed possible shared traits for the clades Pterioidea and Ostreoidea (oysters and relatives) and the first anatomical description of tentacles in Spondylidae (thorny oysters) and Pinnidae (pen shells). Left, tentacle innervation and ciliary tufts; center, tentacle musculature; right, tentacle cilia.

Graphical Abstract Text

Detailed microscopy analysis of mantle tentacles in pteriomorphian bivalves not only provided anatomical evidence to infer the functional morphology of such diverse organs, including sensory roles, mucociliary transportation, and protective functions, but also revealed possible shared traits for the clades Pteriidae and Ostreidae (oysters and relatives) and the first anatomical description of tentacles in Spondylidae (thorny oysters) and Pinnidae (pen shells). Left, tentacle innervation and ciliary tufts; center, tentacle musculature; right, tentacle cilia.

For Peer Review



Candidate image for journal cover. Middle fold tentacle of *Ostrea equestris* showing ciliary tufts and innervation in green (anti- α -tubulin), and nuclei in blue (DAPI).